[1.]Loganathan PARASURAMAN, [2.]Deepa KRISHNAMURTHY

PRANDTL BOUNDARY LAYER FLOW OF A CASSON NANOFLUID PAST A PERMEABLE VERTICAL PLATE

[1-2.]Department of Mathematics, College of Engineering, Guindy, Anna University, Chennai-25, Tamilnadu, INDIA

Abstract: This paper demonstrates the non-Newtonian flow behavior of a nanofluid under the permeability of a porous medium. In particular, this investigation focused on the flow properties of Silica (SiO_2) nanofluid subject to the buoyancy driven Casson fluid flow. The volume fraction of nanoparticles influences the velocity and temperature field. The higher percentage of volume fraction thickens the thermal boundary layer which in turn reduces the growth of velocity boundary layer. The effects of rheological parameters such as Prandtl number, thermal Grashof number, permeability, Casson parameter, Nusselt number and skin friction coefficient has been explored abundantly. The quantitative comparison of this study with the already existing results produces an excellent correlation.
Keywords: Casson fluid; Moving vertical plate; Silica; Nanofluid; Porous medium

INTRODUCTION

Non-Newtonian fluids are processed under laminar flow conditions owing to their high consistency. The wide ranges of applications are found in the non-Newtonian fluids which unveil a pseudoplastic flow. In other words, the fluid exhibits a decrease in viscosity with increasing rate of shear. The paint, printing inks and disperse systems are the most renowned examples of this kind of flow behavior. However, on account of poor flow at low shear rate, the pseudoplasticity is objectionable in some way [Cross (1965)].

The yield stress of a non-Newtonian fluid involves in the rheological characteristics. A substance driven by a yield stress and generating a nonlinear flow curve is often called as the yield-pseudo plastic material. This type of material exhibits infinite apparent viscosity with zero shear rate. At very low apparent viscosity, the rate of shear drastically achieves an infinite value. This viscoplastic behavior associated with the Casson fluid model. Consequently, Casson fluid is described as a non-Newtonian shear thinning fluid with a yield stress. Also, this model has been used for expounding the shear stress and shear rate behaviour of blood, yoghurt, tomato puree, molten chocolate, many food stuffs and biological materials [Chhabra and Richarson (1999)].

The Casson flow model was invented by Casson. The constitutive equation which is formulated for this model is used to effectively illustrate the flow curves for suspension of pigments in printing inks and silicon suspensions. By virtue of its possible applications, many researchers made their focus of attention on this flow model. Hussanan et al. (2014) derived the exact solution of Newtonian heating Casson fluid over an oscillating vertical plate. The notable conclusion of this article is that an increase in the value of Prandtl number and Casson fluid parameter regulate the flow separation. Venkatesan et al. (2014) developed a numerical modelling of Casson fluid through a mild bell shaped stenosis at lower shear rates. It was analyzed that the larger blood vessel with the elevated rate of shear demonstrates the Newtonian characteristics of the fluid; whereas the smaller diameter arteries uplift the apparent viscosity and betraying the non-Newtonian characteristics.

Over the years, nanofluids drew attention of many scientists. Choi initiated the term called nanofluid; accordingly nano technology based heat transfer was evolved [Das et al. (2007), Choi et al. (1995)]. Silica nanofluids have enormous findings in the literature. Generally, this kind of fluid serves as a flow agent in powdered foods and pharmaceutical products. Hydrated silica can be utilized as a rough material in removal of plaques. Theoretically, Blasius and Sakiadis problem for nanofluids was explained by Ahmad et al. (2011). Das et al. (2015) examined the hall current and thermal radiation effects on a water based nanofluid containing Al_2O_3, Cu and Ag nanoparticles under rotating frame of reference over an oscillating porous plate. Noghrehabadi et al. (2011) and Noghrehabadi et al. (2012) inspected the heat transfer enhancement in SiO_2 water nanofluid under the variation of volume fraction and compared the results with Ag water nanofluid over a stretching sheet.

According to Shi et al. (2017), the thermal resistance of miniature heat pipe radiators was lowered for the 0.6% volume fraction of SiO_2 water nanofluid and this nanofluid has strengthen the performance of radiators comparing to the results of DI (Deionized) water. Ullah et al. (2016) studied the effects of chemical reaction and thermal radiation on MHD free convective Casson nanofluid flow past a nonlinearly stretching sheet saturated in a porous medium with slip and convective boundary conditions. Casson nanofluid flow through a cone which is rotated and fixed in a rotating frame filled with ferrous nanoparticles was numerically studied by Raju and Sandeep (2017). Haq et al. (2014) concentrated on the MHD effects with suction/injection of Casson nanofluid past a shrinking sheet and the numerical results were discussed for the flow properties. Meybodi et al. (2015) centralized their priority to viscosity. Least squares support vector machines method is adopted to predict the viscosity in this analyzes. Muthucumaraswamy et al. (2011) found the exact solution of incompressible viscous fluid flow over an oscillating plate with thermal radiation and chemical reaction. Rayleigh's problem described the fluid flow along a moving horizontal plate. On account of practical applications, convective flow over an impulsively started vertical plate has been studied in this article. The most prominent distinctive aspect distinctive aspect of this work is the non-Newtonian flow configuration that has been dealt with the SiO_2 -water nanofluid past a permeable impulsively started semi-infinite vertical plate. The complexities pertaining to the non-linearity of the rheological characteristics are represented graphically. To assure the reliability and accuracy of the solution, the investigation is directed towards the comparison with the results of Soundalgekar (1977). Certainly, the correlation discloses an appreciable and extremely good match.

MATHEMATICAL ANALYSIS

Consider a convective Casson fluid flow over a nanofluid past a permeable moving semi-infinite vertical plate. Assume that the plate is at rest initially. Hence, it is evident that the fluid temperature remains ambient temperature. The plate suddenly starts to accelerate vertically upwards with a constant speed u_0 at $t^* > 0$. This impulsive motion results in the velocity and temperature. At this time level the temperature of the plate raised to $T'_w \ (> T'_\infty)$. Eventually, the fluid encounters the heat transfer near wall. For the case that the flow is far away from the plate, the velocity and temperature gradually drops to zero. The fluid motion is taken along x direction vertically and the y direction is normal to the plate. The velocities u and v are described along vertical and horizontal directions respectively. The schematic representation is shown in figure 1.

The effect of viscous dissipation is negligible in the energy balance equation. The expression for the flow configuration of Casson fluid can be defined by a constitutive relation [Makanda et al. (2015), Arthur et al. (2015), Raju et al. (2016) and Ullah et al. (2016)].

$$\tau_{ij} = \begin{cases} 2\left(\mu_B + \dfrac{P_y}{\sqrt{2\pi}}\right)e_{ij}, & \pi > \pi_c \\ 2\left(\mu_B + \dfrac{P_y}{\sqrt{2\pi_c}}\right)e_{ij}, & \pi \le \pi_c \end{cases}$$

Here, $\pi = e_{ij}e_{ij}$ and e_{ij} is the *(i, j)*th component of the shear rate. π_c is the critical value of π concerned with the model. μ_B is the plastic dynamic viscosity and P_y is the yield stress of the fluid.

The governing boundary layer equations of the mathematical model that encompasses the above assumptions, constitutive equation, Boussinesq approximation and the flow equations mentioned in [Tiwari et al. (2007)] can be expressed as

$$\frac{\partial u}{\partial t^*} = \frac{\mu_{nf}}{\rho_{nf}}\left(1+\frac{1}{\beta}\right)\frac{\partial^2 u}{\partial y^2} + g\frac{(\rho\beta^*)_{nf}}{\rho_{nf}}(T'-T'_\infty) - \frac{\mu_{nf}}{k\rho_{nf}}u \tag{1}$$

$$\frac{\partial T'}{\partial t^*} = \frac{k_{nf}}{(\rho c_p)_{nf}}\frac{\partial^2 T'}{\partial y^2} \tag{2}$$

Suitable initial and boundary conditions of the problem are

$$\begin{aligned} &t^* \le 0,\ u = 0, T' = T'_\infty \quad \text{for all } y \\ &t^* > 0,\ u = u_0, T' = T'_w \quad \text{for } y = 0 \\ &u \to 0, T' \to T'_\infty \quad \text{as } y \to \infty \end{aligned} \tag{3}$$

where β^* is the thermal expansion coefficient, μ_{nf} and ρ_{nf} are the dynamic viscosity and density of nanofluid respectively.

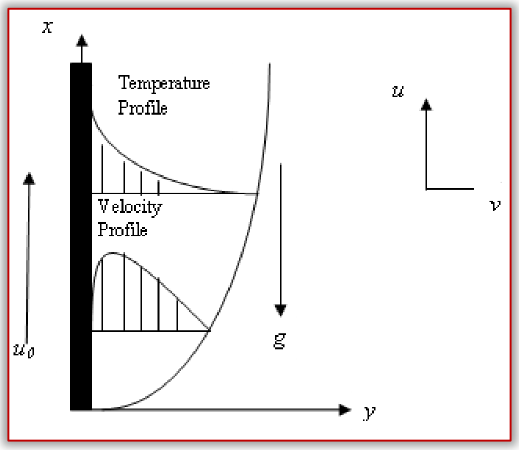

Figure 1. Schematic representation of the flow model

The expressions for the nanofluid parameters are defined as [Ahmad et al. (2011)]

$$\mu_{nf} = \frac{\mu_f}{(1-\phi)^{2.5}},\ \rho_{nf} = (1-\phi)\rho_f + \phi\rho_s,$$
$$(\rho c_p)_{nf} = (1-\phi)(\rho c_p)_f + \phi(\rho c_p)_s,$$
$$(\rho\beta^*)_{nf} = (1-\phi)(\rho\beta^*)_f + \phi(\rho\beta^*)_s$$

Effective thermal conductivity is described by [Oztop et al. (2008), Hamilton and Crosser (1962)]

$$\frac{k_{nf}}{k_f} = \frac{(k_s+2k_f)-2\phi(k_f-k_s)}{(k_s+2k_f)+\phi(k_f-k_s)}$$

Here ϕ is the volume fraction coefficient, ρ_s is the nanoparticle density, ρ_f is the density of the base fluid, $(c_p)_f$ and $(c_p)_s$ are respectively the heat capacity of base fluid and nanoparticle. The thermophysical properties of various materials at 25°C are taken from [Hussein et al. (2013)] and the nanoparticles considered in this investigation are spherical shaped nanoparticles. Non dimensional quantities employed on the coupled partial differential equations (1), (2) and (3) are taken as

$$U = \frac{u}{u_0},\ Y = \frac{yu_0}{\upsilon_f},\ t = \frac{t^* u_0^2}{\upsilon_f},\ T = \frac{T'-T'_\infty}{T'_w - T'_\infty}$$

$$Gr=\frac{\upsilon_f g\beta_f^*(T'_w-T'_\infty)}{u_0^{\,3}},\ Pr=\frac{\upsilon_f(\rho c_p)_f}{k_f},\ K=\frac{ku_0^2}{\upsilon_f^2}$$

where U, Y, t and T are the dimensionless velocity, horizontal direction, time and temperature respectively. Gr is the thermal Grashof number, Pr is the Prandtl number, K is the permeability parameter and υ_f is the kinematic viscosity of the base fluid.

Non dimensional form of (1), (2) and (3) are

$$\frac{\partial U}{\partial t}=\left(1+\frac{1}{\beta}\right)B_1\frac{\partial^2 U}{\partial Y^2}-B_1\frac{U}{K}+B_2 Gr\,T \qquad (4)$$

$$\frac{\partial T}{\partial t}=\frac{1}{Pr}B_3\frac{\partial^2 T}{\partial Y^2} \qquad (5)$$

Appropriate initial and boundary conditions are

$$\begin{aligned} &t\le 0,\ U=0, T=0 \quad \text{for all } Y\\ &t>0,\ U=1, T=1 \quad \text{for } Y=0 \qquad (6)\\ &U\to 0,\ T\to 0 \text{ as } Y\to\infty \end{aligned}$$

Solutions of the equations (4) and (5) together with the initial and boundary conditions (6) are acquired by Laplace transform technique. The expressions which explicate the flow characteristics are obtained as follows.

– Temperature distribution

$$T(Y,t)=\mathrm{erfc}\left[\frac{Y}{2\sqrt{B_3}}\sqrt{\frac{Pr}{t}}\right]$$

– Velocity distribution

Case (i):

If K is finite

$$U(Y,t)=\frac{Gr\,B_2}{B_5}\left\{\begin{array}{l}\frac{e^{B_6 t}}{2}\left[\begin{array}{l}F_1(Y,t)+F_2(Y,t)\\ -F_3(Y,t)-F_4(Y,t)\end{array}\right]\\ -\frac{1}{2}\left[F_5(Y,t)+F_6(Y,t)\right]\\ +\mathrm{erfc}\left(\frac{\sqrt{B_4}\,Y}{2\sqrt{t}}\right)\end{array}\right\}$$

$$+\frac{1}{2}\left[F_5(Y,t)+F_6(Y,t)\right]$$

where
$$F_1(Y,t)=e^{-y\sqrt{\frac{B_5+B_6}{aB_1}}}\ \mathrm{erfc}\left(\frac{Y}{2\sqrt{aB_1 t}}-\sqrt{(B_5+B_6)t}\right)$$

$$F_2(Y,t)=e^{y\sqrt{\frac{B_5+B_6}{aB_1}}}\ \mathrm{erfc}\left(\frac{Y}{2\sqrt{aB_1 t}}+\sqrt{(B_5+B_6)t}\right)$$

$$F_3(Y,t)=e^{-y\sqrt{B_4B_6}}\ \mathrm{erfc}\left(\frac{\sqrt{B_4}\,Y}{2\sqrt{t}}-\sqrt{B_6 t}\right)$$

$$F_4(Y,t)=e^{y\sqrt{B_4B_6}}\ \mathrm{erfc}\left(\frac{\sqrt{B_4}\,Y}{2\sqrt{t}}+\sqrt{B_6 t}\right)$$

$$F_5(Y,t)=e^{-y\sqrt{\frac{B_5}{aB_1}}}\ \mathrm{erfc}\left(\frac{Y}{2\sqrt{aB_1 t}}-\sqrt{B_5 t}\right)$$

$$F_6(Y,t)=e^{y\sqrt{\frac{B_5}{aB_1}}}\ \mathrm{erfc}\left(\frac{Y}{2\sqrt{aB_1 t}}+\sqrt{B_5 t}\right)$$

Case (ii):

As $K\to\infty$, the permeability becomes infinitely large which is the case that there is no porous medium.

$$U(Y,t)=\mathrm{erfc}\left(\frac{Y}{2\sqrt{aB_1 t}}\right)$$

$$+\frac{Gr\,B_2 t}{(aB_1B_4-1)}\left\{\begin{array}{l}\mathrm{erfc}\left(\frac{Y}{2\sqrt{aB_1 t}}\right)-\frac{Y}{\sqrt{\pi aB_1 t}}e^{-\frac{Y^2}{4aB_1 t}}\\ +\frac{Y^2}{2aB_1 t}\mathrm{erfc}\left(\frac{Y}{2\sqrt{aB_1 t}}\right)\\ -\mathrm{erfc}\left(\frac{Y\sqrt{B_4}}{2\sqrt{aB_1 t}}\right)\\ +\frac{Y\sqrt{B_4}}{\sqrt{\pi aB_1 t}}e^{-\frac{Y^2B_4}{4B_1 t}}\\ -\frac{Y^2B_4}{2aB_1 t}\mathrm{erfc}\left(\frac{Y\sqrt{B_4}}{2\sqrt{aB_1 t}}\right)\end{array}\right\}$$

where

$$B_1=\frac{1}{(1-\phi)^{2.5}\left((1-\phi)+\phi\left(\frac{\rho_s}{\rho_f}\right)\right)},\ B_2=\frac{(1-\phi)+\phi\left(\frac{(\rho\beta^*)_s}{(\rho\beta^*)_f}\right)}{(1-\phi)+\phi\left(\frac{\rho_s}{\rho_f}\right)},$$

$$B_3=\frac{k_{nf}}{k_f\left((1-\phi)+\phi\left(\frac{(\rho C_p)_s}{(\rho C_p)_f}\right)\right)}$$

$$B_4=\frac{Pr}{B_3},\ B_5=\frac{B_1}{K},\ B_6=\frac{B_5}{aB_1B_4-1},\ a=1+\frac{1}{\beta}$$

Heat transfer can be analysed from the Nusselt number expression with the various values of Pr.

$$Nu=\frac{k_{nf}}{k_f}\sqrt{\frac{Pr}{\pi B_3 t}}$$

Skin friction coefficient is given by

$$C_f=-\frac{1}{(1-\phi)^{2.5}}\left(1+\frac{1}{\beta}\right)\frac{\partial U}{\partial Y}\bigg|_{Y=0}$$

RESULTS AND DISCUSSION

To establish the validation of the current results, an extensive comparison has been done with the solution of Soundalgekar (1977) for $t=0.2, Pr=0.71, Gr=5\,\&\,10, K\to\infty,\ \beta\to\infty, \phi=0$ and $\eta=\frac{Y}{2\sqrt{t}}$. The exact solution obtained in this study manifests the wonderful match which is illustrated in figure 2.

Figure 3 demonstrates the effects of K, t, Pr and Gr on the velocity of SiO_2 nanoparticles with the fixed volume fraction $\phi=0.02$. The rise in the permeability leads to the increase in velocity. Physically, this is due to the bulk behaviour of the fluid which is strongly depending on the porous medium structure. Velocity is uplifted by the larger time level due to the impulsive motion of the plate with constant velocity. The higher values of Prandtl numer exhibit decrease in the velocity boundary layer as a result of resistance in the fluid flow caused by the viscosity. The greater external cooling of the plate improves the flow speed.

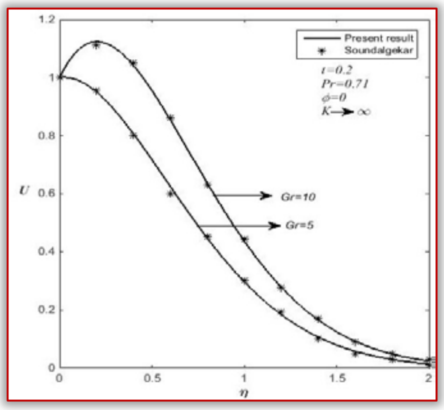

Figure 2. Comparison of velocity profiles with the results of Soundalgekar (1977)

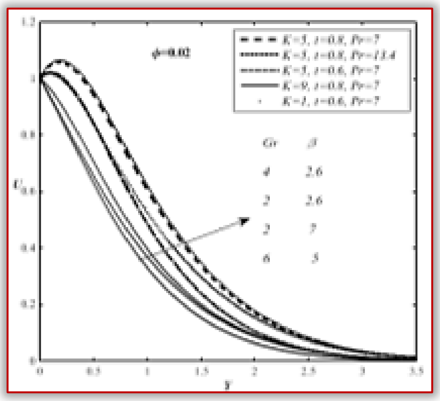

Figure 3. Influence of K, t, Pr, Gr and β on velocity distribution of SiO_2

As mentioned previously, the Casson parameter depends on the viscosity and yield stress of the fluid. By lowering the yield stress, the rise in the values of Casson parameter achieved. This fluid flow resembles the Newtonian fluid flow in default of the yield stress. From figure 3 and 4 the complexities occur in the velocity distribution as a result of elevation in β has been illustrated. Chhabra and Richardson (1977) pointed out that the physical properties of non-Newtonian fluids are normally temperature dependent. The temperature difference is likely to be important in improving the Gr values. The greater values of Gr and β evidently increase the non linearities of the flow curve.

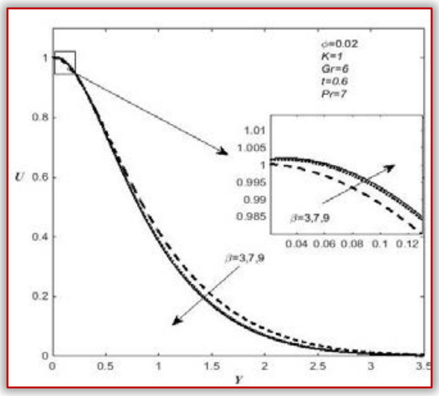

Figure 4. Velocity distributions of SiO_2 for different values of Casson parameter

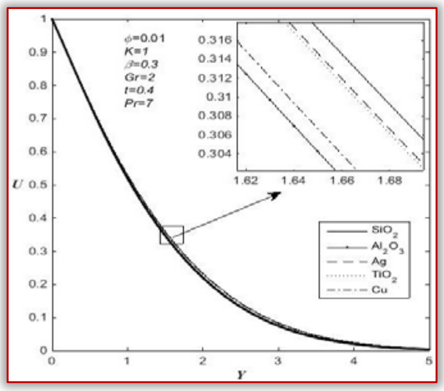

Figure 5. Velocity distributions of various nanoparticles

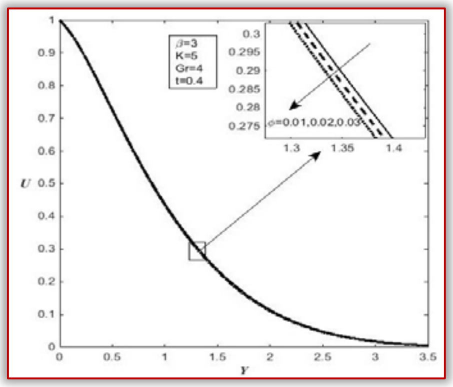

Figure 6. Effect of ϕ on velocity distribution

In figure 5 and 7, the velocity and temperature profiles of various nanoparticles SiO_2, Al_2O_3, Ag, TiO_2 and Cu are discussed. SiO_2 nanoparticles produce the highest velocity distribution and the lowest temperature distribution.

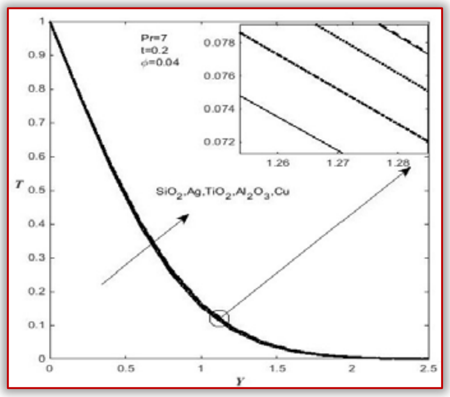

Figure 7. Temperature distribution of various nanoparticles

Figure 8 explains the influence of Prandtl number, ϕ and time. Increasing the values of Prandtl number, results in the temperature drop. This is because of the less physical strength in the thermal conductivity. On the other hand, temperature shoots up rapidly for the elongated time.

Rise in the amount of nanoparticle concentration elevates the thermal conductivity of the base fluid. Due to high thermal conductivity, the thinner momentum boundary layer and thicker thermal boundary layer are observed. These circumstances reduce the speed of the flow and increase the temperature in SiO_2 nanofluid which is depicted in figure 6 and 8.

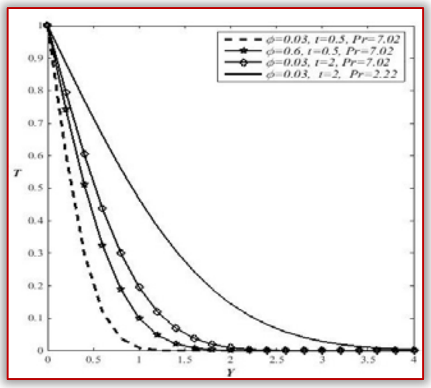

Figure 8. Influence of ϕ, t and $\Pr$ on temperature distribution of SiO_2

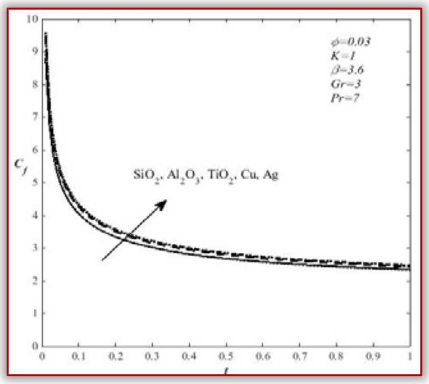

Figure 9. Skin friction coefficient for different nano particles

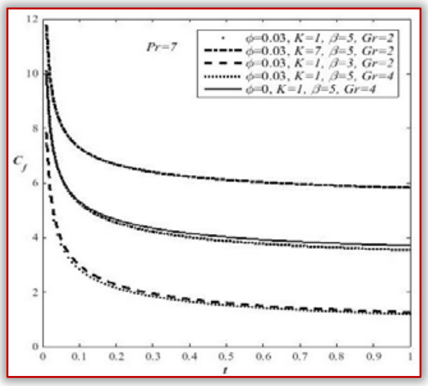

Figure10. Influence of ϕ, K, β and Gr on Skin friction coefficient of SiO_2

The shear stress of the flow towards the plate experiences the velocity gradient and fluid flow retardation. From figure 9, SiO_2 nanoparticles exhibit the lowest skin friction comparing to the other nanoparticles on account of viscosity fluctuation at 3% volume fraction, $K = 1, \beta = 3.6, Gr = 3$ and $\Pr = 7$.

Figure 10 depicts the influence of different parameters on the skin friction coefficient. Thermal conductivity of the conventional fluid greatly improved when the large amount of nanoparticles dispersed. Consequently, there is a drop in the viscous drag. Rise in the permeability leads to the increase in the number of pores or the size of pores in the porous medium. Owing to this fact, the fluid approaches the plate surface easily which improves the friction between the plate and the fluid. An increase in the Grashof number results in the elevation of skin friction coefficient. Higher values of Casson parameter display the growth in viscous drag due to the significant change in dynamic viscosity.

Figure 11 emphasizes the influence of Nusselt number on SiO_2 nanoparticles with 2% volume fraction and Prandtl number values enhance the energy transport from high temperature region to low temperature region. Thus it is evident that there is a remarkable increase in the Nusselt number values.

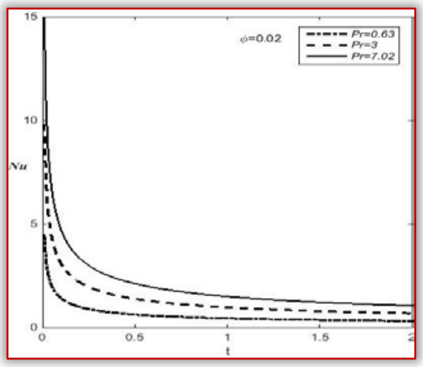

Figure 11. Variation in the Nusselt number in SiO_2 for different $\Pr$

CONCLUSIONS

A bulk of theoretical and experimental investigation carried out on nanofluids. However, very few researchers reviewed the SiO_2 –water nanofluids. In addition to that there is no contribution in non-Newtonian (Casson fluid) behaviour of nanofluids through a porous medium. This study analyses this phenomena and concludes with the following stupendous inferences.

— Among the five nanoparticles including metallic and non-metallic nanoparticles, SiO_2 displays the highest velocity, lowest skin friction and temperature.
— Enhancing Prandtl number values produce the greatest improvement in the Nusselt number but lessen the temperature and velocity field.
— Uplifting Grashof number and Casson parameter provides some irregularities in the flow pattern. Near to the plate surface, it is noted that the velocity is growing and it is decaying while the fluid far away from the surface.
— Volume fraction of nanoparticles (amount of nanoparticles dispersed in the conventional fluid) escalate the temperature and slow down the speed.
— Velocity and temperature field rapidly increases for a large time scale.
— The flow speed is stimulated when the permeability is getting larger. Increment in K, β and Gr display the rise in viscous drag. When there is an increase in the volume fraction coefficient, the skin friction is significantly reduced.

Acknowledgement

One of the authors, K. Deepa immensely expresses the gratitude to Anna University, Chennai for supporting this research work with the financial assistance through "Anna Centenary Research Fellowship".

References

[1] Ahmad, S; Rohni, A.M; Pop, I; Blasius and Sakiadis problems in nanofluids: Acta Mech, Vol.218, pp.195–204, 2011.
[2] Arthur, E.M; Seini, I.Y and Bortteir, L.B; Analysis of Casson fluid flow over a vertical porous surface with chemical reaction in the presence of magnetic field: Journal of Applied Mathematics and Physics, Vol.3, pp.713-723, 2015.
[3] Chhabra, R.P. and Richardson, J.F: Non-Newtonian flow in the process industries; fundamentals and engineering applications, Butterworth-Heinemann publishing, 1999.
[4] Choi, U.S.S. and Eastman, J.A: Enhancing thermal conductivity of fluids with nanoparticles, ASME International Mechanical engineering congress & Exposition, San Francisco, CA, 1995.
[5] Cross, M.M: Rheology of non-Newtonian fluids: A new flow equation for pseudo plastic systems, Journal of colloid science, Vol. 20, pp.417-437, 1965.
[6] Das, S.K; Choi, U.S.S; Yu, W and Pradeep, T: Nanofluids science and technology, A John Wiley & Sons, Inc., Publication, 2007.
[7] Das, S; Jana, R.N, Makinde, O.D: Magnetohydrodynamic free convective flow of nanofluids past an oscillating porous flat plate in a rotating system with thermal radiation and hall effects, Journal of Mechanics, pp.1-14, available at: doi:10.1017/jmech.2015.49, 2015.
[8] Hamilton, R.L and Crosser, O.K: Thermal conductivity of heterogeneous two component systems, I & EC fundamentals, Vol.1 No.3, 1962.
[9] Haq, R.U; Nadeem, S; Khan, Z.H and Okedayo, T.G: Convective heat transfer and MHD effects on Casson nanofluid flow over a shrinking sheet, Central European Journal of Physics, Vol.12 (12), pp.862-871, 2014.
[10] Hussanan, A; Salleh, M.Z; Tahar, R.M and Khan, I: Unsteady boundary layer flow and heat transfer of a Casson fluid past an oscillating vertical plate with Newtonian heating, PLOS ONE, VoL.9(10), 2014.
[11] Hussein, M.A; Bakar, R.A; Kadirgama, K and Sharma, K.V: Experimental measurement of nanofluids thermal properties, International Journal of automotive and mechanical engineering, Vol.7, pp.850-863, 2013.
[12] Makanda, G; Shaw, S and Sibanda, P: Effects of radiation on MHD free convection of a Casson fluid from a horizontal circular cylinder with partial slip in non-Darcy porous medium with viscous dissipation, Boundary Value Problems, Vol.75, 2015.
[13] Meybodi, M.K; Naseri, S; Shokrollahi, A; Daryasafar, A: Prediction of viscosity of water-based Al_2O_3, TiO_2, SiO_2 and CuO nanofluids using a reliable approach, Chemometrics and Intelligent Laboratory Systems, Vol.149, pp.60-69, 2015.
[14] Muthucumaraswamy, R; Nagarajan, G; Subramanian, V.S.A: Thermal radiation and MHD effects on flow past a vertical oscillating plate with chemical reaction of first order, Acta Technica Corviniensis-Bulletin of Engineering, 2011.
[15] Noghrehabadi, A; Ghalambaz, M and Ghalambaz, M: A Theoretical investigation of SiO_2-water nanofluid heat transfer enhancement over an isothermal Stretching sheet, International journal of multidisciplinary sciences and engineering, Vol.2(9), 2011.
[16] Noghrehabadi, A; Ghalambaz, M; Ghalambaz, M and Ghanbarzadeh, A: Comparing thermal enhancement of Ag-water and SiO_2-water nanofluids over an isothermal stretching sheet with suction or injection, Journal of computational and applied research in mechanical engineering, Vol.2(1), pp.37-49, 2012.
[17] Oztop, F.H; Abu-Nada, E: Numerical study of natural convection in partially heated rectangular enclosures filled with nanofluids, International Journal of Heat and Fluid Flow, Vol.29, pp.1326-1336, 2008.
[18] Raju, C.S.K and Sandeep, N: Unsteady Casson nanofluid flow over a rotating cone in a rotating frame filled with ferrous nanoparticles: A numerical study, Journal of Magnetism and Magnetic Materials, Vol.421, pp.216-224, 2017.
[19] Raju, C.S.K; Sandeep, N; Sugunamma, V; Jayachandra Babu, M and Ramana Reddy, J.V: Heat and mass transfer in magnetohydrodynamic Casson fluid over an exponentially permeable stretching surface, Engineering Science and Technology, An International Journal,Vol.19, pp.45-52, 2016.
[20] Shi, J; Zhao, W; Li, J and Liu, Z: Heat transfer performance of heat pipe radiator with SiO_2/Water nanofluids, Heat transfer-Asian research, Vol.46(7), 2017.
[21] Soundalgekar, V.M: Free convection effects on the stokes problem for an infinite vertical plate, Journal of Heat Transfer, Vol.99, pp.499-501, 1977.
[22] Tiwari, R.K; and Das, M.K: Heat transfer augmentation in a two-sided lid-driven differentially heated square cavity utilizing nanofluids, International Journal of Heat and Mass Transfer, Vol.50, pp.2002-2018, 2007.
[23] Ullah, I; Khan, I and Shafie, S: MHD natural convection flow of Casson nanofluid over nonlinearly stretching sheet through porous medium with chemical reaction and thermal Radiation, Nanoscale research letters, Vol.11, 2016.
[24] Ullah, I; Bhattacharyya, I; Shafie, S and Khan, I: Unsteady MHD mixed convection slip flow of Casson fluid over nonlinearly stretching sheet embedded in a porous medium with chemical reaction, thermal radiation, heat generation/absorption and convective boundary conditions, PLOS ONE, 2016.
[25] Venkatesan, J; Sankar, D.S; Hemalatha, K and Yatim, Y: Mathematical analysis of Casson fluid model for blood rheology in stenosed narrow arteries, Journal of Applied Mathematics, Hindawi, 2014.

ACTA TECHNICA CORVINIENSIS BULLETIN OF ENGINEERING
ISSN: 2067-3809